MULTIPARAMETER MICROWAVE RETRIEVAL ALGORITHMS: PART B: PERFORMANCE OF NEURAL NETWORKS

R.M. Gairola*, Estelle Obligis, Emmanuel Moreau, Cecile Mallet and Laurence Eymard
CETP, 10-12 avenue de l'Europe, 78140 Vélizy, France

MEGHA-TROPIQUES 2nd Scientific Workshop, 2-6 July 2001, Paris, France.

Abstract

The present study deals with a new empirical-retrieval algorithm based on the neural network approach introduced for the retrieval of geophysical parameters like wind speed, columnar water vapor and columnar liquid water simultaneously for TRMM-TMI configuration. ECMWF analysis were used for the constitution of the database for radiative transfer simulations of brightness temperatures matching with the ECMWF geophysical input parameters. The results shows that the neural network algorithm has the capacity to outperform the conventional multiple regression for the retrievals of all the three parameters. Since the neural network is highly sensitive to the input data base, we have done some radiative transfer simulations and comparisons over the global tropics by two separate models (named as UCL and other CETP) so as to ascertain one for future retrieval and applications of the geophysical parameters to be obtained from the MADRAS sensor of the MEGHA-TROPIQUES over the tropical regions.

1. Introduction:

There are two major objectives of this paper. The first is to develop a retrieval algorithm for non-raining oceanic and atmospheric parameters like wind speed, water vapor and liquid water etc. to a desired accuracy that should be better or atleast equal to those existing for sensors like SSM/I and TRMM-TMI. The second objective is to ascertain a radiative transfer model for the ocean surface and non-raining atmospheres suitable for the MADRAS sensor applications of MEGHA-TROPIQUES. Part A of this paper, deals with a methodology for the formulation of multi-parameter and multi-instrument retrieval by Obligis et al. (2001).

Recently; artificial neural networks have been recognized as being useful for retrieval operations in remote sensing of the atmosphere. The use of neural network in statistical estimation is often effective because they can simultaneously address nonlinear dependencies and complex statistical behavior. It has been shown that a multilayer perceptron (Beale and Jackson, 1990) with a single hidden layer and nonlinear activation functions is capable of approximating any real valued continuous function, provided a sufficient number of units within the hidden layer exists (Hornik et al. 1989). Several studies have been conducted earlier, for the retrieval of sea surface wind (Goodberlet et al. 1989), total precipitable water (Alishouse et al. 1990a) and integrated cloud liquid water (Alishouse et al. 1990b, Karstens et al. 1994, Gérard and Eymard 1998) using mainly SSM/I data and multiple regression approach. The performance of neural

*Presently on deputation from Department of Space, ISRO Space Applications Centre (Ahmedabad), India.

network approach compared to the multiple regression have recently been shown by Mallet et al. (2001), Jung et al. (1998) and a host of others, for the retrieval of water vapor and liquid water. These studies have demonstrated that neural network out-performs any of the conventional methods for retrievals. All these previous studies form a strong basis for the present attempt to evaluate the performance of neural network and regression approach for TRMM-TMI radiometric channel simulations and retrievals. Part A of this study uses the multiple regression and the present one is based on the neural network approach. In the present paper, we develop algorithms for the retrieval of the geophysical parameters over the oceans mainly, the wind speed (WS), water vapor content (TPW), and cloud/rain liquid water content (CLW) for the TRMM-TMI radiometric channels using a NN approach based on a multilayer perceptron developed by Moreau et al. (2000). These studies will allow an assessment of both the algorithms for future applications related to MADRAS channels.

2. Data Base:

As described in part A of this study, that the main input data base for the radiative transfer simulations comes from a set of ECMWF analysis, representing all the season and regions of the globe. About 25,368 atmospheric profiles between 60 S and 60 N are used for the simulations. The horizontal resolution of these data are 1.125 x 1.125 in latitude and longitude, which corresponds to a 125-km horizontal mesh at the equator and 125 cos0-km mesh at latitude 0. The atmospheric profiles constitutes the temperature, specific humidity, cloud liquid water content vertical profiles defined on 31 levels and the pressure, temperature and specific humidity at the surface and 10-m wind speed. Both UCL and CETP radiative transfer models are used for simulations. Both the models accounts for absorption in the atmosphere and emissivity of wind-roughened sea surface as described in part A of this study. The model does not account for scattering by liquid hydrometeors. However, as an initial experiment with the neural networks, the CETP radiative transfer model simulations over the GI78 data base are utilized for the training and testing purposes, and the summary of the characteristics of each data base is given in Table 1 of Part A of this study.

3. Comparison of Radiative Transfer Models:

Both the CETP and UCL models use the Liebe MPM model (1993) for gaseous absorption by oxygen and water vapor, and Rayleigh theory for absorption by cloud liquid water. The UCL model was originally developed by Guissard and Sobieski (1987) and recently improved by Lemaire (1998), using a double scale emissivity model. The CETP model was developed by Prigent (1990) based on a geometric optics approach and recently improved and validated by Boukabara (1997). The simulations are performed for the TRMM-TMI configuration and the results of comparison are shown in Table. 1. There are quite good agreements of both the models except in lower frequencies. This was as expected, as the UCL model takes into account the small structures like, capillary waves, small gravity waves, superimposed on the large undulations of gravity waves and the scattering coefficients are expressed as the sum of two contributions. While the CETP model considers the sea surface as a set of flat surfaces, with a bi-directional slope distribution. Each facet is considered as an infinite plane regarding the wavelength, so the contribution from the ripples is not taken into account. The lower frequencies in microwaves are important for the determination of surface wind speed and sea surface temperature (SST). Thus even without any calibration and validation, we expect UCL model to perform better for these parameters here based on the theoretical considerations. However, a detailed study is followed to ascertain this aspect and till then the CETP radiative transfer model simulations are being attempted as the input vectors for the ANN approach in the present study.

TABLE 1.

STATISTICS OF INPUT DATA BASE SIMULATIONS

	Min.	Max.	Average	Sigma
Water Vapor	0.120	7.420	2.620	1.578
Liquid Water	0.000	248.030	11.207	16.174
Wind Speed	1.010	26.780	7.561	3.734
Sea Surface Temp.	273.299	304.649	291.347	9.090

STATISTICS OF SIMULATED DATA BASE

	CETP Model				UCL Model			
	Min.	Max.	Ave.	Sigma	Min.	Max.	Ave.	Sigma
TB (10 GHz-V)	157.89	190.91	168.44	5.60	158.55	192.05	169.61	6.00
TB (10 GHz-H)	79.45	136.00	94.26	6.28	89.57	137.05	100.63	5.39
TB (18 GHz-V)	173.85	245.77	197.90	13.94	173.13	245.50	197.46	14.07
TB (18 GHz-H)	94.30	219.34	137.00	20.92	102.43	219.64	141.26	20.16
TB (21 GHz-V)	178.00	266.07	217.07	20.72	177.34	265.95	216.81	20.92
TB (37 GHz-V)	201.96	272.92	220.85	11.90	201.31	272.62	220.67	11.96
TB (37 GHz-H)	122.16	264.60	165.30	20.95	130.95	264.60	169.71	20.21
TB (85 GHz-V)	231.31	285.64	262.68	13.80	231.50	285.17	262.46	13.75
TB (85 GHz-H)	160.14	282.14	234.52	28.91	165.64	282.60	236.52	27.68

4. Retrievals of Parameters:

Given an accurate and reliable radiative transfer model, geophysical retrieval algorithms can be developed. As stated earlier, we are developing in parallel two types of algorithms: multiple linear regression and neural network approach. The radiative transfer simulations by CETP for TMI channels from 10 to 85 GHz has been used here for these analysis, with the statistical characteristics of database given in Table 1 above. Though the neural network is a growing field in itself, a brief description, relevant for this paper is given below:

4.1 The Neural Network Algorithm:

An artificial neural network (ANN) may be viewed as a mathematical model composed of many no-linear computational elements, named neurons, operating in parallel and massively connected by links characterized by different weights. A single neuron computes the sum of its inputs, adds a bias term, and drives the result through a generally nonlinear activation function to produce a single output termed the activation level of the neuron. ANN models are mainly specified by the network topology, neuron characteristics, and training or learning rules (Lippman, 1987). The term topology refers to the architecture of the network as a whole: the number of its input, output and hidden units and their interconnection. For this study, a three layer feedforward neural network is used. It mainly consists of three layers of fully connected nodes. As stated earlier, each hidden or output node in the network receives a "signal" from each node in a previous layer; these signals are summed and are fed in an activation function to produce a single output signal for that node (Fig. 1).

Fig. 1.

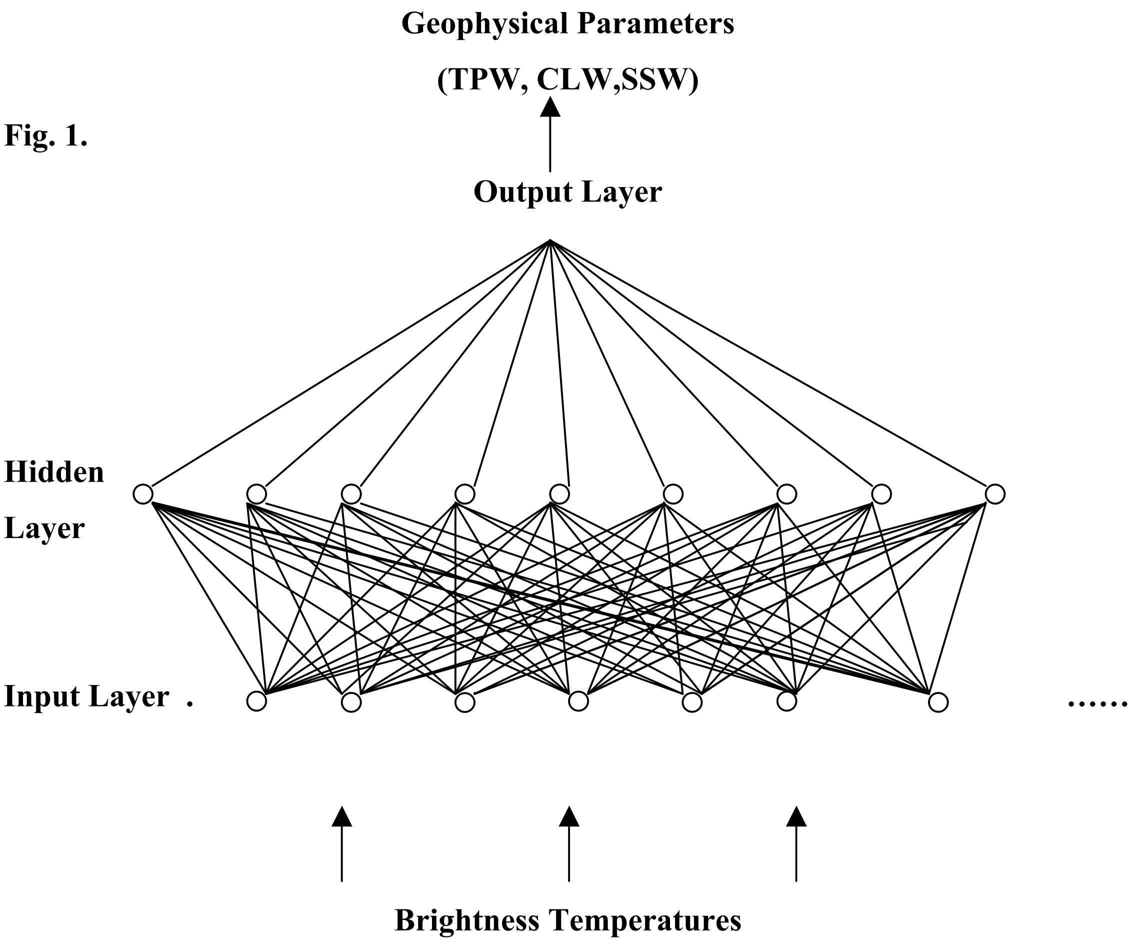

The sigmoid function was chosen as the activation function for all the nodes in the hidden layer, given by

$$f(x) = 1 / (1 + e-x)$$

The sigmoid activation function squashes the input which may have values between plus and minus infinity, to yields these values in the range [0,1]. The multilayer perceptron is designed to approximate an unknown input output relation by determining the weight and strength of each connection via learning rules. These rules indicate how to pursue minimization of the error function measuring the quality of the network's approximation on the restricted domain covered by a training set. In present case the error minimization is done using the back propagation algorithm (Rumelhart et al. 1986), which uses a gradient search technique and iteratively adjusts the weight coefficients in the network to minimize an error function equal to mean square difference between the desired and the actual net output.

5. Results and Discussions:

From the database composed of the simulated brightness temperatures (TB) for the TMI configuration and water vapor, liquid water and SST from the corresponding atmospheric profiles, a ANN algorithm is applied to derive the weights and the residual error of the algorithms. The training cycle involved forward feeding TB values in the training set from the input layer to the output layer to calculate the three mapping errors associated with total water vapor, cloud liquid water content and surface wind speed separately and then backward propagating the mapping errors from the output layer to the input layer by adjusting the weights in the ANN. The root mean square error is calculated after all the input and output pairs in the training set are processed. The training is stopped in all the three cases when the rms error converged to a specified rms tolerance. A total of 25368 input data base constituting of the 9 simulated TB's from 10 to 85 GHz and the corresponding output data of water vapor, liquid water and wind speed were used, out of which 20000 were used in training and rest for testing the algorithm in all the three cases. All the three parameters achieved best performance of the ANN with different architecture and number of iterations for three parameters. The analysis of the results are presented below for each parameters separately.

5.1 Total Precipitable Water:

Fig 2a shows the distribution of error with number of iterations during learning (continuous line) and testing phase (dotted line). It is evident that in case of water vapor the error drops very

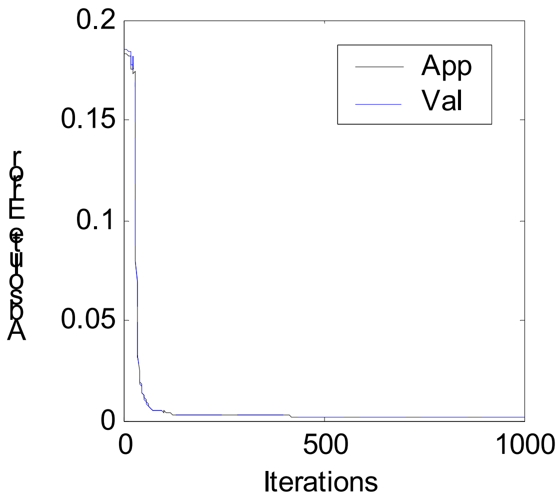

Fig. 2a: Distribution of Global Errorr

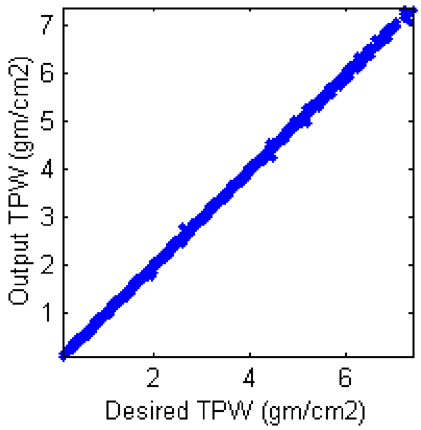

Fig. 2b: Desired vs. ANN Retrieved TPW for Learning Data

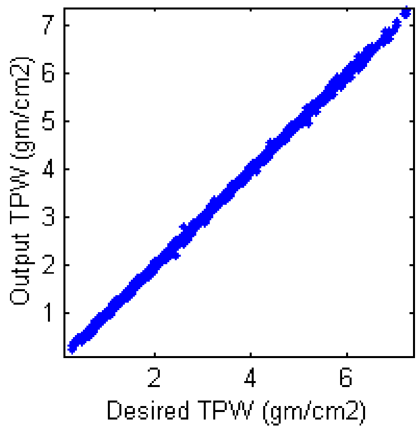

Fig. 2c: Desired vs. ANN Retrieved TPW for Testing Data

sharply within a few hundred iterations and later becomes almost constant. The Fig 2(b,c) shows the corresponding distribution of the desired water vapor versus the ANN retrieved water vapor for learning (2000) and testing (5368) data sets respectively. The error statistics of these data distribution are shown in Fig. 2(c, d) for the similar learning and testing data sets respectively. The correlation coefficient was found 0.99 in both cases and the rms error and bias was 0.031 and 0.032 respectively. These are very encouraging results and thus allow us to look for the running error estimates (i.e; the bias, standard deviation and rms error respectively) for each bins of water vapor for both learning and testing sets of data in Fig. 2(e,f). During the learning phase, the rms error and sd are highest above 3.5 gm/cm2 and the bias peaks at around 3.8 and above 6 gm/cm2 of water vapor content. However these values of error estimates are very marginal and the average error estimates shown in Fig. 2(b,c) could be considered statistically representative and very significant for both learning and testing cases.

Fig. 2d: Data distribution & error statistics (for training data sets)

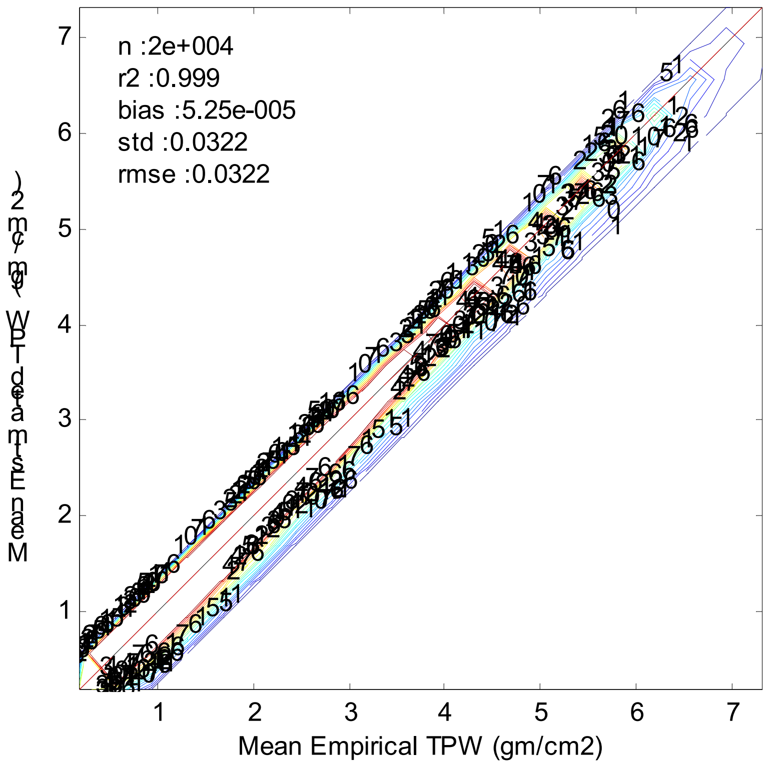

Fig. 2e: Data distribution & error statistics (for testing data sets)

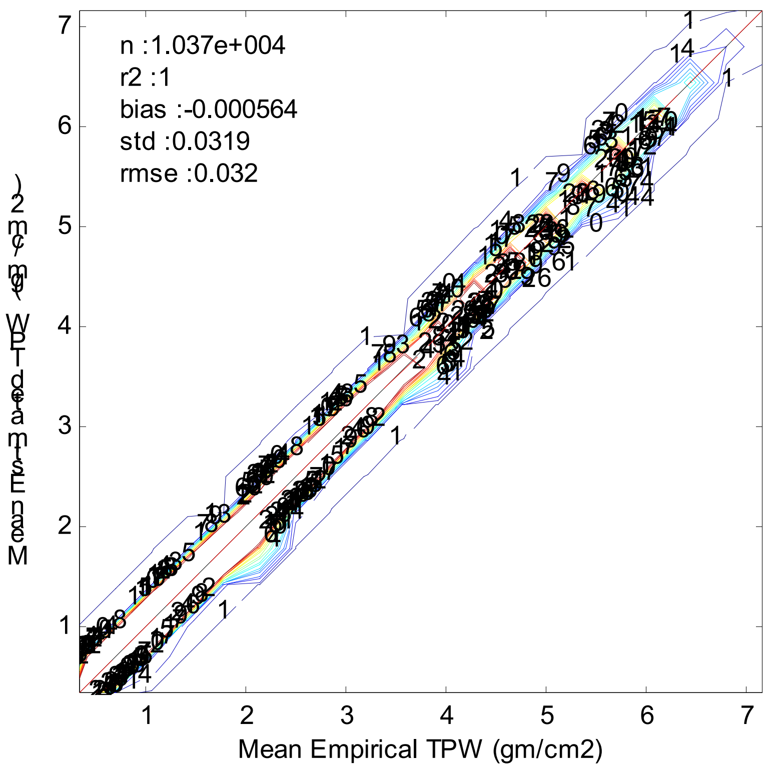

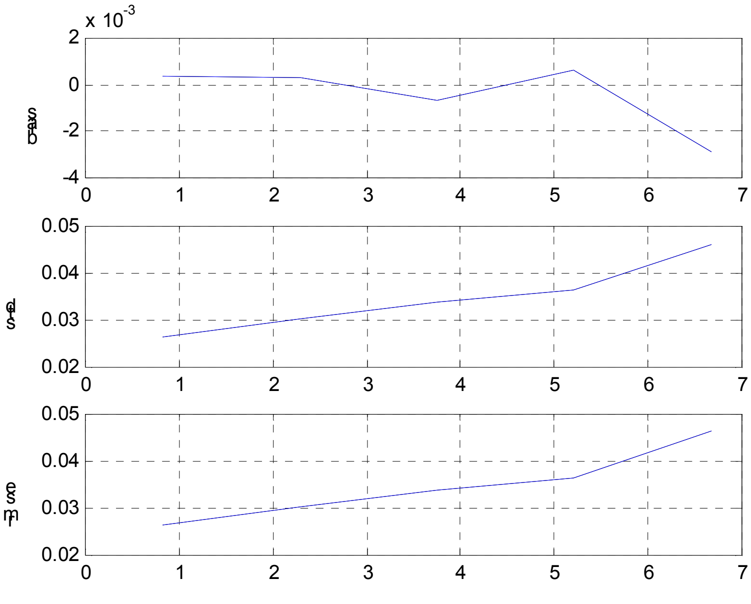

Fig 2f: Binned TPW (gm/cm2) (for training data set)

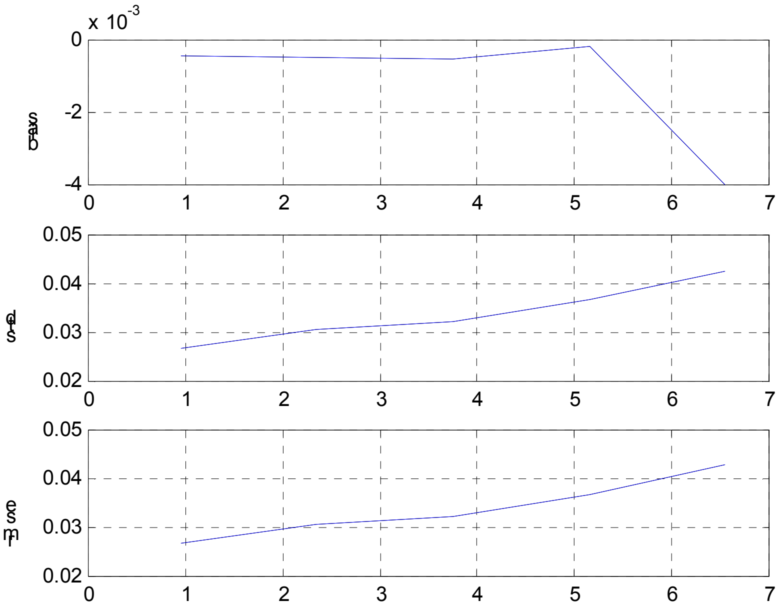

Fig 2g: Binned TPW (gm/cm2) (for testing data set)

5.2 Cloud Liquid Water Content:

Similar experiment has been performed for the cloud liquid water content to evaluate the performance of ANN. The dynamic range of liquid water in ECMWF fields were found from 0 to 248.03 mg/cm2. However, above 80 mg/cm2 could be considered normal raining to very heavy raining situations. Thus the results of radiative transfer simulations for the ECMWF profiles with liquid water content only upto 80 gm/cm2 are taken for consideration in ANN learning and testing procedures. Similar as above for water vapor, the time evolution of error during the training and testing phase are shown in Fig. 3a with the continuous and dotted lines respectively which seems to be going parallel due to the equal representativity of the data in both learning and testing data sets. A high correlation coefficient of 0.99 and rms error less than 0.9 mg/cm2 in both cases is a very encouraging result for liquid water which has a very nonlinear response to brightness temperatures. The scatter and contour plot of the desired and retrieved values are shown in Fig. 3(b,c). The binned bias, SD and rms errors are also shown in Fig. 3(d,e) respectively which are all mutually statistically consistent and very encouraging.

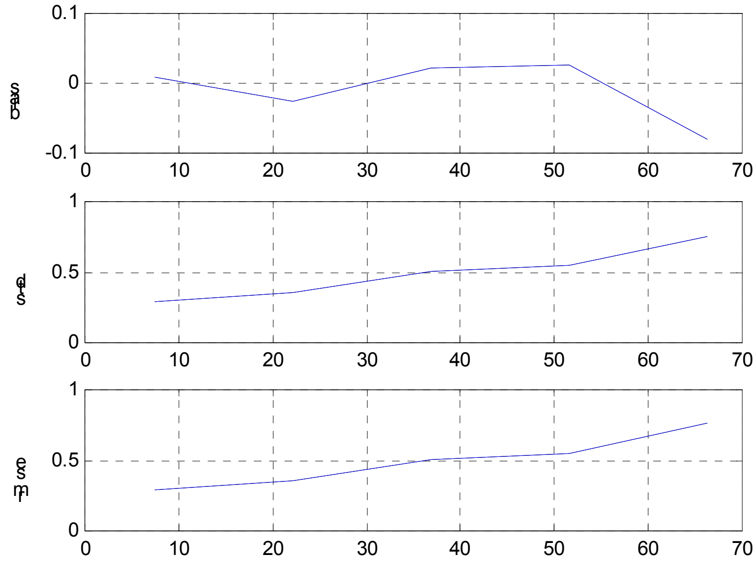

Fig. 3a: Binned CLW (mg/cm2) (for training data sets)

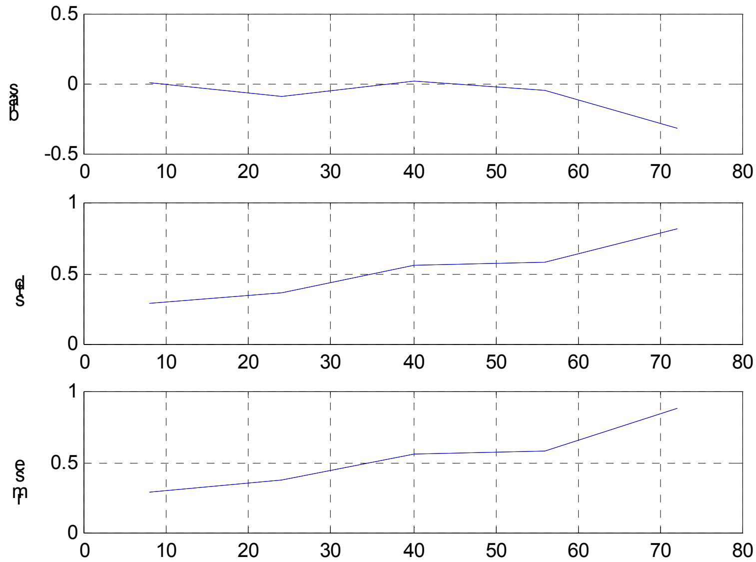

Fig. 3b: Binned CLW (mg/cm2) (for testing data sets)

5.3 Surface Wind Speed:

While not specifically designed as a wind retrieval instrument, the scanning radiometer aboard TRMM, the TMI, has made it possible to examine the benefits of 10 GHz band to radiometric wind estimates. The TMI uses the same collection of brightness temperature channels as SSM/I with addition of vertically and horizontally polarized channels at 10 GHz. This channel provides a more transparent window to the ocean surface, while still maintaining sensitivity to the wind modulated ocean surface brightness temperatures. However, this channel is not going to be available with the MADRAS sensor, but the attempts are made to estimate the capability of ANN for the wind retrievals here with TMI configuration and simulations thereof. For brevity

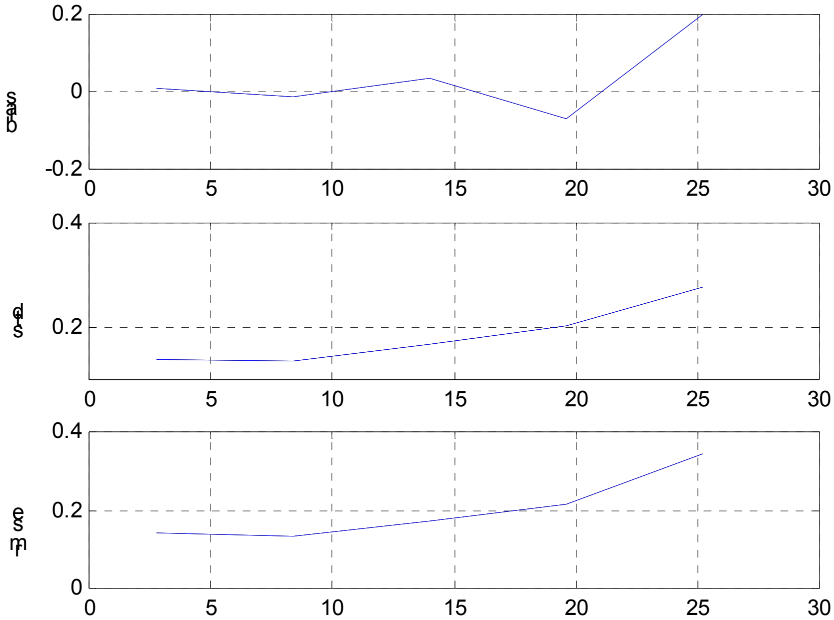

Fig. 4a: Binned Wind Speed (m/s) (for training data sets)

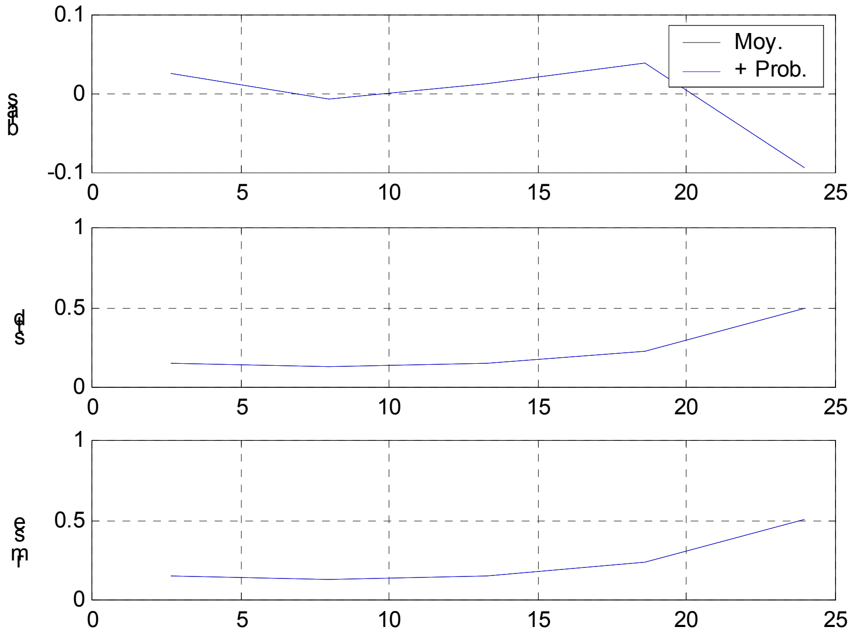

Fig. 4b: Binned Wind Speed (m/s) (for testing data sets)

only the figures for the error statistics and their running distributions are shown in Fig. 4 (a, b) and 4(c, d) respectively. A correlation coefficient of 0.998 is found in both learning and testing cases. The bias and rms error are minimum upto 18 m/sec. Initially all the channel combinations of 37 GHz and below are opted as the input vectors. The optimization of channel combination is being performed with more sensitivity experiments. Still the results in all the three cases are highly encouraging to look forward for the ANN approach to be adopted for the retrieval from MADRAS observations with the other existing methods.

Acknowledgements:

The first author would like to thank CNRS for providing opportunity to work with CETP, Velizy and CNES for sponsoring this work under the Indo-French Program on MEGHA-TROPIQUES during the course of this study.

References:

Alishouse, J.C., Snyder, S.A., Vongsathorn, J. and Ferraro, R.R., Determination of oceanic total precipitable water from SSM/I, IEEE Trans. Geosci. Remote Sens., 28, 811-816, 1990a.

Beale, R., and T. Jackosn, Neural computing, An introduction, Adam Hilger, Bristol, England, 1990.

Boukabara, S.-A. “Couplage des mesures hyperfréquences actives et passives“, Thèse de doctorat de l’Université Paris7, 1997.

Gérard E. and L. Eymard, Remote sensing of integrated cloud liquid water: Development of algorithms and qulity control.

Goodberlet, M.A., C.T. Swift, and J.C. Wilkerson, Remote sensing of ocean surface winds with the Special Sensor Microwave/Imager, J. Geophys. Res. 94, 14,547-14,555, 1989.

Guissard A. and P. Sobieski, “An approximate model for the microwave brightness temperature of the sea“, Int. J. Remote Sens., 8, pp. 1607-1627, 1987.

Hornik, K., M. Stinchombe, and H. White, Multilayer feed forward networks are universal approximators, Neural Networks, 2, 359-366, 1989.

Jung, T., Ruprecht, E. and F. Wagner, Determination of cloud liquid water path over the oceans from SSM/I data using neural networks, Jour. Appl. Met. 37, 832-844, 1998.

Karstens, U., C. Simmer, and E. Ruprecht, Remote sensing of cloud liquid water, Meteorol. Atmos. Phys., 54, 157-171, 1994.

Lemaire D., “Non-fully developed sea state characteristics from real aperture radar remote sensing“, Ph. D. Thesis, Université Catholique de Louvain, Faculté des Sciences Appliquées, 220 pp., 1998.

Lippmann, R.P., An introduction to computing with neural nets, IEEE ASSP Mag., 4, 4-22, 1987.

Mallet C., Moreau E., Casagianole L. Klapisz. C.,: Determination of integrated cloud liquid water path and total precipitable water from SSM/I data using a neural network algorithm, Int. Jour. Remote Sensing, Accepted 1999.

Moreau E., Mallet C., Thiura S., Mabboux B., Clapisz C.: Atmospheric liquid water retrieval using a Gated Expert Neural Network, JTECH Accepted 2001.

Moreau E., Restitution de paramètres atmosphériques par radiométrie hyperfréquence spatiale .Utilisation de méthodes neuronales, Ph.D. Thesis. 2000.

Obligis E., L. Eymard, and R.M. Gairola, Multiparameter retrieval algorithms. part a : forward modeling and performance of multi-linear regression 2001, This Volume.

Prigent C., and P. Abba, “Sea surface equivalent brightness temperature at millimeter wavelength“, Annales Geophysicae, 8, pp. 627-634, 1990.

Rumelhart, D.E., G.E. Hinton, and R.J. Williams, Learning internal representations by error propagation, in Parallel Distributed Processing, edited by, D.E. Rumelhart and J.L. McClelland, pp. 318-362, MIT Press, Cambridge, Mass., 1986.